Title

The genetic landscape of anaplastic pleomorphic xanthoastrocytoma

Journal

Brain Pathology, 29(1)

ISSN

1015-6305

Authors

Phillips, Joanna J

Gong, Henry

Chen, Katharine

et al.

Publication Date

2019

DOI

10.1111/bpa.12639

Peer reviewed

Article Type: Research Article

The genetic landscape of anaplastic pleomorphic xanthoastrocytoma

Joanna J. Phillips[1,2,3,*], Henry Gong[1], Katharine Chen[1], Nancy M. Joseph[4,5], Jessica van Ziffle[4], Boris C. Bastian[3,4], James P. Grenert[4,5], Cassie N. Kline[6], Sabine Mueller[1,6], Anuradha Banerjee[6], Theodore Nicolaides[1,6], Nalin Gupta[1,3], Mitchel S. Berger[1,3], Han S. Lee[2], Melike Pekmezci[2], Tarik Tihan[2], Andrew W. Bollen[2,3], Arie Perry[1,2,3], Joseph T.C. Shieh[9,10], David A. Solomon[2,3,4]

[1]Department of Neurological Surgery, University of California San Francisco, San Francisco, CA

[2]Division of Neuropathology, Department of Pathology, University of California San Francisco, San Francisco, CA

[3]Helen Diller Family Comprehensive Cancer Center, University of California San Francisco, San Francisco, CA

[4]Clinical Cancer Genomics Laboratory, University of California San Francisco, San Francisco, CA

[5]Department of Pathology, University of California San Francisco, San Francisco, CA

[6]Division of Pediatric Hematology/Oncology, Department of Pediatrics, University of California San Francisco, San Francisco, CA

[9]Department of Pediatrics, Division of Medical Genetics, University of California San Francisco, San Francisco, CA

[10]Institute for Human Genetics, University of California, San Francisco, CA

*Corresponding author:

University of California San Francisco

Department of Neurological Surgery

Helen Diller Family Cancer Building, HD492B

San Francisco, CA 94143
Phone 415-514-4929
FAX 415-514-9792
joanna.phillips@ucsf.edu

Acknowledgements: This study was funded in part by the UCSF Department of Pathology, UCSF Brain Tumor SPORE Tissue Core (NIH/NCI P50 CA097257), the Pediatric Brain Tumor Foundation (J.J.P and T.N.), NIH/NINDS R01 (NS081117, J.J.P.), and NIH Director's Early Independence Award (DP5 OD021403, D.A.S.). We would like to thank the UCSF Department of Neurosurgery Brain Tumor SPORE Tissue Core for biospecimens, and Anny Shai, Yunita Lim, and Gayane Koshkakaryan for their technical help. We also thank and acknowledge the patients and families affected by PXA for their generous contributions to these studies.

ABSTRACT

Pleomorphic xanthoastrocytoma (PXA) is an astrocytic neoplasm that is typically well circumscribed and can have a relatively favorable prognosis. Tumor progression to anaplastic PXA (WHO grade III), however, is associated with a more aggressive biologic behavior and worse prognosis. The factors that drive anaplastic progression are largely unknown. We performed comprehensive genomic profiling on a set of twenty-three PXAs from 19 patients, including 15 with anaplastic PXA. Four patients had tumor tissue from multiple recurrences, including two with anaplastic progression. We find that PXAs are genetically defined by the combination of *CDKN2A* biallelic inactivation and *RAF* alterations that were present in all 19 cases, most commonly as *CDKN2A* homozygous deletion and *BRAF* p.V600E mutation but also occasionally *BRAF* or *RAF1* fusions or other rearrangements. The third most commonly altered gene in anaplastic PXA was *TERT*, with 47% (7/15) harboring *TERT* alterations, either gene amplification (n=2) or promoter hotspot mutation (n=5). In tumor pairs analyzed before and after anaplastic progression, two had increased copy number alterations and one had *TERT* promoter mutation at recurrence. Less commonly altered genes included *TP53*, *BCOR*, *BCORL1*, *ARID1A*, *ATRX*, *PTEN*, and *BCL6*. All PXA in this cohort were IDH and histone H3

wildtype, and did not contain alterations in *EGFR*. Genetic profiling performed on six regions from the same tumor identified intratumoral genomic heterogeneity, likely reflecting clonal evolution during tumor progression. Overall, anaplastic PXA is characterized by the combination of *CDKN2A* biallelic inactivation and oncogenic RAF kinase signaling as well as a relatively small number of additional genetic alterations, with the most common being *TERT* amplification or promoter mutation. These data define a distinct molecular profile for PXA and suggest additional genetic alterations, including *TERT*, may be associated with anaplastic progression.

Keywords: anaplastic PXA, TERT promoter mutations, intratumoral heterogeneity, pediatric glioma, glioma progression

INTRODUCTION

Pleomorphic xanthoastrocytoma (PXA) is an astrocytic neoplasm that most often presents in children or young adults but can also occur in adults (13, 32). While the majority of tumors at presentation are WHO grade II tumors, a subset either present or recur with anaplastic features and are thus designated anaplastic PXA, WHO grade III (12). Overall PXA has a reported prognosis of 67% survival at 10 years (32); however, development of anaplastic PXA is associated with a significant reduction in overall survival (15).

The diagnosis of anaplastic PXA is made based upon tumor histopathologic characteristics and requires increased proliferative activity (mitotic index $\geq$ 5 mitoses/10 HPF), which is associated with worse overall survival (15). In general, anaplastic PXAs acquire features of a more aggressive astrocytic neoplasm that can include increased proliferation, necrosis, microvascular proliferation, loss of pericellular reticulin, and increased infiltrative growth (15, 21). The acquisition of these aggressive biologic behaviors suggests potential genetic evolution in these tumors. Yet, intratumoral genetic heterogeneity, an indication of tumor evolution (3, 14), has not previously been studied in anaplastic PXA.

The activating *BRAF* p.V600E (c.1799T>A) mutation is a common genetic alteration in both PXA and anaplastic PXA, identified in approximately 65% of tumors (15, 36, 49). *BRAF* p.V600E mutations are common in several cancers, including low

grade gliomas, melanoma, thyroid, and colon cancer (8–10, 36), in which they drive activation of the mitogen-activated protein kinase (MAPK) signaling pathway (9, 46). Identification of the mutation can be important as BRAF V600E mutant protein can be targeted therapeutically by small molecule inhibitors of both RAF (e.g. vemurafenib) and MEK (e.g. trametinib). In addition, PXAs commonly harbor homozygous deletion of the *CDKN2A* tumor suppressor (encoding both p16 and p14) on chromosome locus 9p21.3 (45, 47). Across all pediatric gliomas, the combination of *BRAF* mutation and *CDKN2A* homozygous deletion is common in low-grade tumors that transform to high-grade and is associated with poor response to current adjuvant therapies (25, 30). Other genetic alterations recurrently seen in pediatric and adult diffuse gliomas have not been reported in anaplastic PXA, such as alterations in *SETD2*, *H3F3A*, *HIST1H3B*, *EGFR*, *PDGFRA*, *FGFR1*, *PIK3CA*, and *PTEN* (5, 6, 40, 49).

Advances in molecular characterization of central nervous system neoplasms seek to improve tumor classification and therapeutic outcome (11, 16, 36, 37, 39, 43). Indeed, recent changes in the 2016 WHO Classification of Tumours of the Central Nervous System incorporate histopathologic and molecular features for diagnosis of several entities (28). Currently, anaplastic PXA is diagnosed based solely on histopathologic features. Yet recent reports based on DNA methylation data suggest anaplastic PXA-like tumors can masquerade as GBM (24) and epithelioid GBM (1, 23). Importantly these PXA-like tumors were associated with a more favorable prognosis than GBM and included both *BRAF* p.V600E mutant and non-mutant tumors in approximately equal proportions (24). These findings suggest both histologic analysis and determination of *BRAF* p.V600E mutation status may not capture all tumors with the biologic behavior of anaplastic PXA. Indeed, in-frame gene fusions involving RAF kinase family members can drive MAPK signaling and have been identified in PXA lacking *BRAF* p.V600E mutations (33).

Despite progress in our understanding of certain molecular events in PXA, currently there are no molecular markers associated with anaplastic progression. In this study we ask whether tumors that have undergone anaplastic progression share specific features or characteristic genetic alterations. We performed genomic profiling on tumors from 15 patients with anaplastic PXA of which 4 had tumor samples from multiple

recurrences and one had six anatomically distinct samples from a single tumor. Of the four cases with multiple resections, two had anaplastic progression.

MATERIALS AND METHODS

Case selection and histology. A total of 23 cases were identified based upon submission for clinical testing or from review of records in the UCSF Brain Tumor Research Center Biorepository and the Department of Pathology, Division of Neuropathology at the University of California San Francisco. Each case was reviewed and diagnosed as part of their diagnostic work-up at UCSF, which included review by one senior neuropathologist (A.P., A.W.B., or T.T.), and all cases were re-reviewed by two expert neuropathologists (J.J.P. and D.A.S). In addition, diagnostically challenging cases were reviewed by a consensus group of neuropathologists (A.P., A.W.B., T.T., and D.A.S.) with a uniform consensus diagnosis of PXA or anaplastic PXA established for all included cases. The distinction between PXA (WHO grade II) and anaplastic PXA (WHO grade III) was based upon the grading criteria of ≥5 mitoses per 10 high power fields as stated in the 2016 WHO Classification (28). A summary of the histologic features for each of the cases is presented in **Supplementary Table 1**, including presence or absence of eosinophilic granular bodies, infiltrative growth, pericellular reticulin deposition, perivascular inflammatory infiltrate, OLIG2 expression, mitotic activity, Ki-67 labeling index, p16 expression, necrosis, microvascular proliferation, and leptomeningeal extension. Immunohistochemical assessment was performed using antibodies against: neurofilament (NF) protein (Cell Marque predilute (clone #2F11), Rocklin, CA), MIB-1 for Ki-67 (790-4286 Ventana predilute, Ventana Medical Systems, Inc., Tucson, AZ), OLIG2 (Immuno Biological Laboratories Co., Ltd., Japan), and p16 (E6H4, Ventana Medical Systems, Inc., Tucson, AZ). Digital photomicrographs were taken using an Olympus DP72 camera.

Genetic evaluation. DNA was extracted from formalin-fixed, paraffin-embedded (FFPE) or flash-frozen tissue using the QIAamp DNA FFPE Tissue Kit (Qiagen) according to the manufacturer's protocol. Genomic DNA was extracted from peripheral blood (15/19) and tumor tissue (23/23). A minimum of 60% tumor nuclei, based on H&E review, was required for DNA extraction. Capture-based next-generation sequencing

(NGS) was performed at the UCSF Clinical Cancer Genomics Laboratory to target and analyze the coding regions of 510 cancer-related genes, *TERT* promoter, select introns from 40 genes to enable detection of structural variants including gene fusions, and DNA segments at regular intervals along each of chromosomes to enable genome-wide copy number analysis, with a total sequencing footprint of 2.8 Mb (UCSF500 Cancer Panel). Sequencing libraries were prepared from genomic DNA with target enrichment performed by hybrid capture using a custom oligonucleotide library (Roche Nimblegen). Sequencing of captured libraries was performed on an Illumina HiSeq 2500. Duplicate sequencing reads were removed computationally to allow for accurate allele frequency determination and copy number estimates (41). The analysis was performed using the following software packages: BWA, Samtools, Picard tools, GATK, CNVkit, Pindel, SATK, Annovar, Freebayes, Delly, and Nexus Copy Number Biodiscovery. Single nucleotide variants (SNVs), small indels, and structural rearrangements were visualized individually using Integrated Genome Viewer (IGV) and reference genome assembly GRCh37/hg19. For somatic SNVs and small indels, we required high quality variants, coverage of >50 total reads and absence in the germline. For this platform, samples with at least 25% tumor, ≥ 200x coverage for the tumor sample, and ≥ 100x coverage for the normal sample, the detection sensitivity is 99% and 83% and the specificity is 98% and 71% for fully clonal SNVs and small indels, respectively, and the sensitivity of detection of copy number changes is 100%. Large insertions, deletions, and copy number alterations were visualized using IGV and Nexus Copy Number.

Ethics statement. The ethics approval number for the use of de-identified human biospecimens and autopsy material is 10-01318. These studies were in accordance with the ethical standards of the institutional research committee and with the 1964 Helsinki declaration and its later amendments. This article does not contain any studies with animals.

RESULTS

Clinical-pathologic features. Patient clinical characteristics and tumor WHO grade is summarized in **Figure 1**. We identified 23 tumors, including 15 anaplastic PXA (WHO grade III), from a total of 19 patients. In the cohort of patients with anaplastic PXA, the median age at initial diagnosis was 24 years (range 9-74), and tumors were primarily supratentorial 94% (14/15) with 40% (6/15) involving the temporal lobe. In patients with anaplastic PXA, median follow-up was 3.2 years from disease diagnosis (range 0.3-17.6 years, n=12) and two patients had died of their disease (**Supplemental Figure 1a**). Overall, 92% (12/13) had recurred with a median recurrence-free survival from first diagnosis of 1.3 years (range 0.5-6.7 years) (**Supplemental Figure 1b**). In the majority of cases leptomeningeal disease was noted (7/10). In the four patients with PXA lacking anaplastic features, median follow-up was 3.3 years from disease diagnosis (range 0.2-14.5 years, n=4) and two had recurred (**Supplemental Figure 1a-b)**.

All tumors demonstrated characteristic features of PXA (**Figure 2, left column**), including pleomorphic, spindled, or sometimes focal epithelioid neoplastic cells with astrocytic morphology, pericellular reticulin, often eosinophilic granular bodies, primarily solid, non-infiltrative growth pattern highlighted by a relative lack of neurofilament-positive neuronal processes within the tumor, immunostaining for OLIG2, and relatively low to moderate proliferation (mean mitotic index < 1 mitosis per 10 high power fields, n=4). Anaplastic PXA (**Figure 2, right column**) shared similar features with PXA, including eosinophilic granular bodies, but, in addition, harbored regions with increased proliferation (mean 14.4 mitoses per 10 high power fields, n=11, and mean 15% Ki-67 labeling index, n= 15) and often had tumor regions with loss of pericellular reticulin and increased tumor cell infiltration with entrapped neuropil. The identification of solid growth with a lack of diffuse infiltration, a biphasic tumor with both solid and infiltrative regions, presence of eosinophilic granular bodies, and presence pericellular reticulin was used to establish a diagnosis of anaplastic PXA versus an infiltrative glioma or epithelioid glioblastoma. Anaplastic PXA with or without *BRAF* p.V600E mutation had similar histologic appearance (data not shown). The histopathologic and immunohistologic features of the tumors are summarized in **Supplemental Table 1**.

Somatic variants and copy number alterations. Targeted capture and next-generation sequencing of 510 cancer-associated genes was performed in each sample to identify single nucleotide variants, insertion/deletions (indels), structural variants including gene fusions, and copy number alterations (**Supplemental Table 2**). All nineteen tumors from individual patients harbored alterations in RAF family kinase members. *BRAF* was altered in 89% (17/19) with the activating *BRAF* p.V600E mutation identified in fifteen tumors, one tumor with an in-frame deletion of 15 base pairs within exon 12 of the *BRAF* gene, and one tumor with an *NRF1-BRAF* in-frame gene fusion. The remaining two tumors had structural rearrangements involving *RAF1*, one with an *ATG7-RAF1* in-frame gene fusion and one with a 39 Kb deletion of a segment of chromosome 3p25.2 containing the 5' coding exons of the *RAF1* gene that fuses an upstream intergenic region with exons 8-17 of *RAF1* containing the carboxy-terminal serine/threonine kinase domain (**Supplemental Table 3**). The *NRF1-BRAF* fusion and *ATG7-RAF1* fusion have previously been reported and are associated with activation of MAPK signaling activity (19, 33) and similar small in-frame deletions within exon 12 of *BRAF* have been shown to drive MAPK signaling activity in Langerhans cell histiocytosis lacking *BRAF* p.V600E mutation(7). In tumors from four patients with multiple resections, alterations in RAF family kinase genes and homozygous deletion of the *CDKN2A* locus were retained at each recurrence. Homozygyous/biallelic deletion of the *CDKN2A* locus at 9p21 was identified in 95% (18/19) of tumors. The single remaining tumor had loss of one copy of chromosome 9 without a genetic event affecting the remaining *CDKN2A* allele identified. However, this tumor demonstrated complete absence of immunostaining for p16 protein, suggesting biallelic inactivation of *CDKN2A* through epigenetic silencing (e.g. promoter methylation) or a cryptic genetic alteration not detected by this sequencing assay (2, 34, 44).

After *BRAF* p.V600E mutation and *CDKN2A* homozygous deletion, the most common alteration identified in 47% (7/15) of anaplastic PXA was alteration of the *TERT* gene. Two tumors contained amplification of the *TERT* gene and five tumors harbored a hotspot mutation in the promoter region of *TERT* that is common in glioblastoma, oligodendroglioma, and several other human tumors and results in expression of telomerase reverse transcriptase (TERT) (4, 17). One additional tumor had gain of

chromosome 5p that includes the *TERT* gene (PXA#10). After *TERT*, additional alterations were rare with the most common alterations, occurring in two independent anaplastic tumors each, were known pathogenic mutations in *TP53* (*TP53* p.R273H and p.V225fs), truncating mutations or deletions in *BCOR* or *BCORL1* (*BCOR* homozygous deletion, *BCORL1* p.S55fs,), truncating or missense mutation in *SPTA1* (*SPTA1* p.V982fs and p.T1953I), and focal deletion of *ARID1A* (**Figures 1 and 4, Supplemental Tables 4-5**). Additional likely pathogenic missense mutations were identified in *ATRX*, *PTEN*, *GAB2*, *CBL*, *NF1*, and *NOTCH3*, and *BCL6* (**Supplemental Table 3**). Mutation or amplification of *TERT* and mutation of *ATRX* were mutually exclusive. A single anaplastic tumor, PXA#15, had focal amplification of chromosome 4q12 including *PDGFRA* (**Supplemental Table 5**). Examination of somatic non-synonymous single nucleotide variants, stop gains, splice site, or frameshift insertions/deletions revealed an average of 2.7 alterations total per anaplastic tumor (range 0-7, **Figure 1**). The mean number of alterations in tumors from patients 24 years or younger (1.9) was less than that in tumors from patients older than 24 years (3.6) ($p<0.05$). Several characteristic gene alterations of pediatric and adult infiltrating astrocytoma were not identified, including alterations in *IDH1, IDH2, SETD2, H3F3A*, *HIST1H3B*, *EGFR*, *FGFR1-3*, *ACVR1*, *PPM1D*, *NTRK1-3*, *MYB*, *MYBL1*, and *PIK3CA*.

In addition to copy number alterations involving chromosome 9 and the *CDKN2A* locus, copy number alterations were frequent and involved whole chromosome or whole arm gains, losses, and copy-neutral loss of heterozygosity (CNLOH). Overall, anaplastic PXA harbored a median of 5 altered chromosomes per tumor (range 0-21) and PXA without anaplastic features had a median of 2 altered chromosomes per PXA (range 1-11) ($p=0.3$). The most common alterations in anaplastic tumors included gains involving chromosome 5 (n=7) and 21 (n=7) and losses involving chromosome 9 (n=12) and 10 (n=7) (**Supplemental Table 5**). While the mean number of copy number alterations per tumor was greater in patients older than the median age of 24 at initial diagnosis (10.7 versus 4.1, $p<0.05$), the progression-free survival for patients with 3 or less (3.2 years) versus more than 3 (1.3 years) copy number alterations per tumor was not significantly different. Whole chromosome copy number gains resulted in up to 7 copies of a single

chromosome. While whole loss or copy-neutral loss of heterozygosity of chromosome 10 was common (5/15), focal loss of 10q was not identified.

Anaplastic progression of PXA. Four patients had tumor tissue from multiple recurrences, including two with anaplastic progression from PXA to anaplastic PXA following a subtotal resection (**Figure 3**). In both cases with anaplastic progression there was a marked increase in copy number alterations (**Supplemental Table 5**). In addition, PXA#8r harbored a newly acquired *TERT* promoter mutation (*TERT* g.1,295,228G>A [c.-124C>T], commonly termed *TERT* C228T) while PXA#7r contained a focal deletion of *ARID1A* and a *CBL* p.C384R mutation (**Supplemental Tables 4-5**). Consistent with ongoing genomic evolution of anaplastic PXA over time, acquired alterations at recurrence included focal deletion of *ARID1A* in two tumors, gain of missense mutations or truncating mutations in *NOTCH3* and *NF1*, and increased copy number alterations.

Intratumoral heterogeneity of genetic alterations in anaplastic PXA. Intratumoral heterogeneity of genetic alterations reflects the evolution of genetically distinct subclones that ultimately leads to malignant progression. To investigate the intratumoral heterogeneity in anaplastic PXA, a total of 6 samples were analyzed from anatomically distinct regions of PXA#4, taken at time of autopsy (**Figure 4a**). H&E staining revealed only minimal variation in tumor cell morphology in the different regions, while Ki-67 immunostaining demonstrated increased proliferation in sample 1A at the anterior and inferior most aspect of the resection cavity (**Figure 4b**). All samples contained *NRF1-BRAF* fusion with identical fusion breakpoints, and copy number analysis revealed focal *CDKN2A* homozygous deletion on chromosome 9p21 with identical deletion breakpoints in all 6 samples (**Figure 4c, Supplemental Table 5**). In contrast, copy number loss involving an interstitial portion of chromosome 6q was only present in 3 tumor regions. On average three non-synonymous single nucleotide variants was identified per tumor region (range 1-5) (**Table 1 and Supplemental Table 4**). A variant in the *KEAP1* gene, which encodes Kelch Like ECH Associated Protein 1, located in the BTB domain (p.V79D, NM_012289) was identified in all 6 tumor regions. Despite similar high tumor content of all samples based on the uniformly deep amplitude of the *CDKN2A* homozygous deletion, the mutant allele frequency of the *KEAP1* variant ranged from 3-37%, suggesting that the regions contained different proportions of tumor cells harboring

the *KEAP1* mutation. The remaining somatic mutations were identified regionally and at lower variant allele frequencies than the *KEAP1* variant. Region 1B and 1F shared variants in *FOXO1*, *TNC*, and *MGA*, but did not share additional variants from other areas (**Table 1**). Variants identified in tumor regions 1C, 1D, and 1E were not shared with other regions. Together, these data demonstrate that the *NRF1-BRAF* fusion and *CDKN2A* homozygous deletion were likely to have occurred early in tumor development, while other variants present at subclonal mutant allele frequencies (e.g. *KEAP1* variant) were likely to have occurred later during the course of tumor progression.

DISCUSSION

Anaplastic PXA is associated with a more aggressive clinical course, yet the factors that drive anaplastic progression are unknown. Using capture-based next-generation sequencing of 23 PXA from 19 patients, including fifteen anaplastic PXA, we find that PXAs are genetically defined by the combination of *CDKN2A* biallelic inactivation and *RAF* alterations that were present in all cases. While no generalized recurrent genetic alterations were associated with a more aggressive biologic behavior, 47% (7/15) of anaplastic PXA had alterations of *TERT*, including hotspot mutation in the *TERT* promoter and amplification of the *TERT* gene. In one case *TERT* promoter mutation accompanied anaplastic progression in a matched tumor pair. Given these data in combination with previous reports of *TERT* promoter mutations in a small number of PXA, anaplastic PXA, and epithelioid GBM (17, 20, 23, 29, 31), we suggest alterations in the *TERT* promoter are more common than previously reported and likely contribute to anaplastic progression in PXA. While our cohort of WHO grade II tumors was too small to compare between WHO grade II and grade III tumors, analysis of published reports (17, 20, 23) reveals that *TERT* promoter mutation is more common in PXA with anaplastic features versus PXA without anaplasia (**Supplemental Table 7** and **8**, Fisher's exact test, $p<0.05$, n=37 with *TERT* promoter mutation, n=132 without).

The coexistence of *TERT* promoter and *BRAF* p.V600E mutations has been reported in several cancers, including melanoma and papillary thyroid cancer for which the coexistence of the two mutations is associated with more aggressive disease (26, 38, 48). Mechanistic studies suggest *BRAF* driven MAPK signaling can synergize with *TERT*

promoter mutation to drive oncogenesis (27). Consistent with a potential synergistic oncogenic action involving MAPK signaling, we identified *TERT* alterations in both *BRAF* p.V600E mutant anaplastic PXA (5/11) and tumors with alternate RAF family kinase alterations that lack *BRAF* p.V600E (2/4). While *TERT* alterations were identified across all age groups, *TERT* amplification (n=2) was identified in younger patients while TERT promoter mutation (n=5) was identified in patients 11 years or older. The potential importance of telomere maintenance in PXA is further supported by the identification of a loss of function mutation in *ATRX* in a tumor without *TERT* alterations. Previously, two cases with *ATRX* deletion and one case with activation of the alternative lengthening of telomeres pathway in combination with ATRX protein mislocalization have been reported in anaplastic PXA (35, 45). Additional studies are needed to investigate the prognostic role for *TERT* and *ATRX* alterations in PXA and their potential role in anaplastic progression.

Widespread copy number alterations including gains, losses, and copy neutral loss of heterozygosity (CNLOH) were identified in both PXA and anaplastic PXA. Comparing tumors at initial diagnosis (n=8) to those at recurrence (n=11), there was no significant difference in the number of alterations; however, in three of four matched pairs, we observed an increase in copy number alterations over time. One pair had an initial diagnosis of anaplastic PXA and two pairs progressed from PXA to anaplastic PXA. In conjunction with recent reports, these data indicate that a subset of PXA undergo a period of chromosomal instability during anaplastic progression with acquisition of numerous chromosomal gains and losses (45). In contrast, other PXA show similar chromosomal copy number profiles at recurrence, indicating that recurrence and anaplastic progression in PXA is not always driven by chromosomal instability (45).

In addition to mutations in *BRAF* and *TERT*, there were a small number of less commonly altered genes in anaplastic PXA including *ATRX*, *PTEN*, *TP53*, *BCOR*, *BCORL1*, *ARID1A*, and *BCL6*. Interestingly, focal deletion of *ARID1A* occurred in two matched pairs at recurrence, which appeared to be either subclonal or heterozygous in both cases. Our tumors lacked pathogenic alterations in several genes characteristic of specific pediatric or adult glioma entities, including IDH-wildtype GBM and pediatric subtypes of GBM, which can mimic PXA or anaplastic PXA (1, 23, 24). These included

a lack of alterations in *SETD2*, *H3F3A*, *HIST1H3B*, *HIST1H3C*, *EGFR*, *FGFR1-3*, *ACVR1*, *PPM1D*, *IDH1*, *IDH2*, *CIC*, *FUBP1*, *NTRK1-3*, *MET*, *MYB*, *MYBL1*, *MYCN*, *MDM2*, *MDM4*, *PIK3R1*, and *PIK3CA*. A focal amplification of *PDGFRA* was identified in one anaplastic PXA with an unusual clinical presentation in the cerebellum. The histologic features were classic for anaplastic PXA with pleomorphic multinucleated cells, lipidized cells, fascicular growth, abundant eosinophilic granular bodies, and lack of significant infiltration.

The distinction between anaplastic PXA and epithelioid GBM can be challenging and some authors have speculated that these may be related entities or possibly the same entity (1, 18, 29, 31, 42). A recent genomics study suggested that epithelioid GBM is a histologic pattern of high grade glioma that may represent at least three molecularly and biologically distinct entities, including PXA (23). Epithelioid GBM that clustered by genome-wide methylation analysis with PXA in this study had absence of oncogene amplifications and intact chromosome 10q containing the *PTEN* locus. In our cohort, focal amplification of receptor tyrosine kinase genes including *EGFR*, *PDGFRA*, *MET*, or *FGFR1* was seen in only a single case (PXA #15 with *PDGFRA* amplification) and whole chromosome 10 loss or copy-neutral loss of heterozygosity was seen in five cases. Focal loss of 10q was not identified. Although gain of chromosome 7 was present in six cases and whole loss or copy-neutral loss of heterozygosity of chromosome 10 was present in five cases, the combination of polysomy 7 and monosomy 10 was only present in two cases in this cohort (anaplastic PXA #7, and PXA #18, both of which were highly aneuploid tumors with classic histologic features of PXA, *BRAF* V600E mutation, and *CDKN2A* homozygous deletion). This provides a cytogenetic distinction from the vast majority of IDH-wildtype glioblastomas arising in the cerebral hemispheres of adults that harbor this combination of trisomy 7 and monosomy 10.

Analysis of genetic intratumoral heterogeneity in anaplastic PXA revealed both clonal and subclonal alterations. Oncogenic alterations occurring early in tumor development, homozygous deletion of *CDKN2A* and the *NRF1-BRAF* fusion, were identified in all 6 tumor regions. In contrast, a variant in *KEAP1* (p.V79D) was present at different mutant allele frequencies across tumor regions. In addition, across the different regions of the same tumor several subclonal somatic variants and copy number alterations

were identified. The KEAP1 protein regulates NRF2 (nuclear factor erythroid 2-related factor 2) via ubiquitination. While the *KEAP1* p.V79D variant has not previously been associated with cancer, this amino acid is highly conserved and other alterations in the KEAP1 BTB domain have been associated with constitutive activation of NRF2 in cancer (22). These data demonstrate genetic heterogeneity in anaplastic PXA. The contribution of these variants to tumor evolution and tumor aggressiveness will be of interest for future studies.

In summary, while *BRAF* p.V600E mutant gliomas represent a heterogeneous group of neoplasms, our data confirm that *CDKN2A* homozygous deletion in combination with RAF alterations is a defining genetic feature of PXA and anaplastic PXA. Furthermore, chromosomal copy number alterations are widespread and common. Our data demonstrate that alterations in *TERT* are frequent, identified in 47% (7/15) of tumors, and suggest that several pathways may contribute to anaplastic progression in PXA.

Conflict of Interest: The authors declare that they have no conflict of interest.

REFERENCES

1. Alexandrescu S, Korshunov A, Lai SH, Dabiri S, Patil S, et al. 2016. Epithelioid Glioblastomas and Anaplastic Epithelioid Pleomorphic Xanthoastrocytomas-Same Entity or First Cousins? *Brain Pathol. Zurich Switz.* 26(2):215–23
2. Alves MKS, Faria MHG, Neves Filho EHC, Ferrasi AC, Pardini MI de MC, et al. 2013. CDKN2A promoter hypermethylation in astrocytomas is associated with age and sex. *Int. J. Surg. Lond. Engl.* 11(7):549–53

3. Andor N, Graham TA, Jansen M, Xia LC, Aktipis CA, et al. 2016. Pan-cancer analysis of the extent and consequences of intratumor heterogeneity. *Nat. Med.* 22(1):105–13

4. Bell RJA, Rube HT, Kreig A, Mancini A, Fouse SD, et al. 2015. The transcription factor GABP selectively binds and activates the mutant TERT promoter in cancer. *Science*. 348(6238):1036–39

5. Bettegowda C, Agrawal N, Jiao Y, Wang Y, Wood LD, et al. 2013. Exomic sequencing of four rare central nervous system tumor types. *Oncotarget*. 4(4):572–83

6. Brennan CW, Verhaak RGW, McKenna A, Campos B, Noushmehr H, et al. 2013. The somatic genomic landscape of glioblastoma. *Cell*. 155(2):462–77

7. Chakraborty R, Burke TM, Hampton OA, Zinn DJ, Lim KPH, et al. 2016. Alternative genetic mechanisms of BRAF activation in Langerhans cell histiocytosis. *Blood*. 128(21):2533–37

8. Cohen Y, Xing M, Mambo E, Guo Z, Wu G, et al. 2003. BRAF mutation in papillary thyroid carcinoma. *J. Natl. Cancer Inst.* 95(8):625–27

9. Davies H, Bignell GR, Cox C, Stephens P, Edkins S, et al. 2002. Mutations of the BRAF gene in human cancer. *Nature*. 417(6892):949–54

10. Dougherty MJ, Santi M, Brose MS, Ma C, Resnick AC, et al. 2010. Activating mutations in BRAF characterize a spectrum of pediatric low-grade gliomas. *Neuro-Oncol.* 12(7):621–30

11. Eckel-Passow JE, Lachance DH, Molinaro AM, Walsh KM, Decker PA, et al. 2015. Glioma Groups Based on 1p/19q, IDH, and TERT Promoter Mutations in Tumors. *N. Engl. J. Med.* 372(26):2499–2508

12. Giannini C, Paulus W, Louis DN, Liberski PP, Figarella-Branger D, Capper D. Anaplastic pleomorphic xanthoastrocytoma. In: WHO Classification of Tumours of the Central Nervous System, Louis DN, Ohgaki H, Wiestler OD, CaveneeWK (eds). In *WHO Classification of Tumours of the Central Nervous System*, pp. 98–99. International Agency for Research on Cancer: Lyon

13. Giannini C, Scheithauer BW, Burger PC, Brat DJ, Wollan PC, et al. 1999. Pleomorphic xanthoastrocytoma: what do we really know about it? *Cancer*. 85(9):2033–45

14. Greaves M, Maley CC. 2012. Clonal evolution in cancer. *Nature*. 481(7381):306–13

15. Ida CM, Rodriguez FJ, Burger PC, Caron AA, Jenkins SM, et al. 2015. Pleomorphic Xanthoastrocytoma: Natural History and Long-Term Follow-Up. *Brain Pathol. Zurich Switz.* 25(5):575–86

16. Khuong-Quang D-A, Buczkowicz P, Rakopoulos P, Liu X-Y, Fontebasso AM, et al. 2012. K27M mutation in histone H3.3 defines clinically and biologically distinct subgroups of pediatric diffuse intrinsic pontine gliomas. *Acta Neuropathol. (Berl.).* 124(3):439–47

17. Killela PJ, Reitman ZJ, Jiao Y, Bettegowda C, Agrawal N, et al. 2013. TERT promoter mutations occur frequently in gliomas and a subset of tumors derived from cells with low rates of self-renewal. *Proc. Natl. Acad. Sci. U. S. A.* 110(15):6021–26

18. Kleinschmidt-DeMasters BK, Aisner DL, Birks DK, Foreman NK. 2013. Epithelioid GBMs show a high percentage of BRAF V600E mutation. *Am. J. Surg. Pathol.* 37(5):685–98

19. Kline CN, Joseph NM, Grenert JP, van Ziffle J, Talevich E, et al. 2017. Targeted next-generation sequencing of pediatric neuro-oncology patients improves diagnosis, identifies pathogenic germline mutations, and directs targeted therapy. *Neuro-Oncol.* 19(5):699–709

20. Koelsche C, Sahm F, Capper D, Reuss D, Sturm D, et al. 2013. Distribution of TERT promoter mutations in pediatric and adult tumors of the nervous system. *Acta Neuropathol. (Berl.).* 126(6):907–15

21. Koelsche C, Sahm F, Wöhrer A, Jeibmann A, Schittenhelm J, et al. 2014. BRAF-mutated pleomorphic xanthoastrocytoma is associated with temporal location, reticulin fiber deposition and CD34 expression. *Brain Pathol. Zurich Switz.* 24(3):221–29

22. Konstantinopoulos PA, Spentzos D, Fountzilas E, Francoeur N, Sanisetty S, et al. 2011. Keap1 mutations and Nrf2 pathway activation in epithelial ovarian cancer. *Cancer Res.* 71(15):5081–89

23. Korshunov A, Chavez L, Sharma T, Ryzhova M, Schrimpf D, et al. 2017. Epithelioid glioblastomas stratify into established diagnostic subsets upon integrated molecular analysis. *Brain Pathol. Zurich Switz.*

24. Korshunov A, Ryzhova M, Hovestadt V, Bender S, Sturm D, et al. 2015. Integrated analysis of pediatric glioblastoma reveals a subset of biologically favorable tumors

with associated molecular prognostic markers. *Acta Neuropathol. (Berl.)*. 129(5):669–78

25. Lassaletta A, Zapotocky M, Mistry M, Ramaswamy V, Honnorat M, et al. 2017. Therapeutic and Prognostic Implications of BRAF V600E in Pediatric Low-Grade Gliomas. *J. Clin. Oncol. Off. J. Am. Soc. Clin. Oncol.* 35(25):2934–41
26. Liu R, Bishop J, Zhu G, Zhang T, Ladenson PW, Xing M. 2016. Mortality Risk Stratification by Combining BRAF V600E and TERT Promoter Mutations in Papillary Thyroid Cancer: Genetic Duet of BRAF and TERT Promoter Mutations in Thyroid Cancer Mortality. *JAMA Oncol.*
27. Liu R, Zhang T, Zhu G, Xing M. 2018. Regulation of mutant TERT by BRAF V600E/MAP kinase pathway through FOS/GABP in human cancer. *Nat. Commun.* 9(1):579
28. Louis DN, Perry A, Reifenberger G, von Deimling A, Figarella-Branger D, et al. 2016. The 2016 World Health Organization Classification of Tumors of the Central Nervous System: a summary. *Acta Neuropathol. (Berl.)*. 131(6):803–20
29. Matsumura N, Nakajima N, Yamazaki T, Nagano T, Kagoshima K, et al. 2016. Concurrent TERT promoter and BRAF V600E mutation in epithelioid glioblastoma and concomitant low-grade astrocytoma. *Neuropathol. Off. J. Jpn. Soc. Neuropathol.*
30. Mistry M, Zhukova N, Merico D, Rakopoulos P, Krishnatry R, et al. 2015. BRAF mutation and CDKN2A deletion define a clinically distinct subgroup of childhood secondary high-grade glioma. *J. Clin. Oncol. Off. J. Am. Soc. Clin. Oncol.* 33(9):1015–22

31. Nakajima N, Nobusawa S, Nakata S, Nakada M, Yamazaki T, et al. 2017. BRAF V600E, TERT promoter mutations and CDKN2A/B homozygous deletions are frequent in epithelioid glioblastomas: a histological and molecular analysis focusing on intratumoral heterogeneity. *Brain Pathol. Zurich Switz.*

32. Perkins SM, Mitra N, Fei W, Shinohara ET. 2012. Patterns of care and outcomes of patients with pleomorphic xanthoastrocytoma: a SEER analysis. *J. Neurooncol.* 110(1):99–104

33. Phillips JJ, Gong H, Chen K, Joseph NM, van Ziffle J, et al. 2016. Activating NRF1-BRAF and ATG7-RAF1 fusions in anaplastic pleomorphic xanthoastrocytoma without BRAF p.V600E mutation. *Acta Neuropathol. (Berl.)*

34. Reis GF, Pekmezci M, Hansen HM, Rice T, Marshall RE, et al. 2015. CDKN2A loss is associated with shortened overall survival in lower-grade (World Health Organization Grades II-III) astrocytomas. *J. Neuropathol. Exp. Neurol.* 74(5):442–52

35. Rodriguez FJ, Vizcaino MA, Blakeley J, Heaphy CM. 2016. Frequent alternative lengthening of telomeres and ATRX loss in adult NF1-associated diffuse and high-grade astrocytomas. *Acta Neuropathol. (Berl.).* 132(5):761–63

36. Schindler G, Capper D, Meyer J, Janzarik W, Omran H, et al. 2011. Analysis of BRAF V600E mutation in 1,320 nervous system tumors reveals high mutation frequencies in pleomorphic xanthoastrocytoma, ganglioglioma and extra-cerebellar pilocytic astrocytoma. *Acta Neuropathol. (Berl.).* 121(3):397–405

37. Schwartzentruber J, Korshunov A, Liu X-Y, Jones DTW, Pfaff E, et al. 2012. Driver mutations in histone H3.3 and chromatin remodelling genes in paediatric glioblastoma. *Nature*. 482(7384):226–31

38. Shain AH, Yeh I, Kovalyshyn I, Sriharan A, Talevich E, et al. 2015. The Genetic Evolution of Melanoma from Precursor Lesions. *N. Engl. J. Med.* 373(20):1926–36

39. Sturm D, Orr BA, Toprak UH, Hovestadt V, Jones DTW, et al. 2016. New Brain Tumor Entities Emerge from Molecular Classification of CNS-PNETs. *Cell*. 164(5):1060–72

40. Sturm D, Witt H, Hovestadt V, Khuong-Quang D-A, Jones DTW, et al. 2012. Hotspot mutations in H3F3A and IDH1 define distinct epigenetic and biological subgroups of glioblastoma. *Cancer Cell*. 22(4):425–37

41. Talevich E, Shain AH, Botton T, Bastian BC. 2016. CNVkit: Genome-Wide Copy Number Detection and Visualization from Targeted DNA Sequencing. *PLoS Comput. Biol.* 12(4):e1004873

42. Tanaka S, Nakada M, Nobusawa S, Suzuki SO, Sabit H, et al. 2014. Epithelioid glioblastoma arising from pleomorphic xanthoastrocytoma with the BRAF V600E mutation. *Brain Tumor Pathol.* 31(3):172–76

43. Taylor MD, Northcott PA, Korshunov A, Remke M, Cho Y-J, et al. 2012. Molecular subgroups of medulloblastoma: the current consensus. *Acta Neuropathol. (Berl.)*. 123(4):465–72

44. Ueki K, Ono Y, Henson JW, Efird JT, von Deimling A, Louis DN. 1996. CDKN2/p16 or RB alterations occur in the majority of glioblastomas and are inversely correlated. *Cancer Res.* 56(1):150–53

45. Vaubel RA, Caron AA, Yamada S, Decker PA, Eckel Passow JE, et al. 2017. Recurrent copy number alterations in low-grade and anaplastic pleomorphic xanthoastrocytoma with and without BRAF V600E mutation. *Brain Pathol. Zurich Switz.*

46. Wan PTC, Garnett MJ, Roe SM, Lee S, Niculescu-Duvaz D, et al. 2004. Mechanism of activation of the RAF-ERK signaling pathway by oncogenic mutations of B-RAF. *Cell*. 116(6):855–67

47. Weber RG, Hoischen A, Ehrler M, Zipper P, Kaulich K, et al. 2007. Frequent loss of chromosome 9, homozygous CDKN2A/p14(ARF)/CDKN2B deletion and low TSC1 mRNA expression in pleomorphic xanthoastrocytomas. *Oncogene*. 26(7):1088–97

48. Xing M, Liu R, Liu X, Murugan AK, Zhu G, et al. 2014. BRAF V600E and TERT promoter mutations cooperatively identify the most aggressive papillary thyroid cancer with highest recurrence. *J. Clin. Oncol. Off. J. Am. Soc. Clin. Oncol.* 32(25):2718–26

49. Zhang J, Wu G, Miller CP, Tatevossian RG, Dalton JD, et al. 2013. Whole-genome sequencing identifies genetic alterations in pediatric low-grade gliomas. *Nat. Genet.* 45(6):602–12

FIGURE LEGENDS

Figure 1. Clinical and genomic landscape of anaplastic pleomorphic xanthoastrocytoma (PXA). Clinical and genomic features of 15 anaplastic PXA (left) and 4 PXA (right). Tumors are arranged by age from young to old (from left to right) within each tumor grade and the percent of anaplastic tumors with the alteration are noted on the right for *BRAF*, *RAF1*, *CDKN2A/B*, and *TERT*. Progression-free survival (PFS)

and overall survival (OS) from the time of initial diagnosis and the patient status at last follow-up are indicated.

Figure 2. Histologic features of PXA. Characteristic features of PXA, WHO grade II (left column), including pleomorphic, spindled, or focal epithelioid neoplastic cells with astrocytic morphology, pericellular reticulin, primarily solid, non-infiltrative growth pattern highlighted by lack of neurofilament, and relatively low to moderate proliferation (mean mitotic index < 1 mitosis per 10 high power fields, n=4) Anaplastic PXA, WHO grade III (right column), shares many features with PXA but, in addition, areas can lack pericellular reticulin, exhibit infiltrative growth (entrapped axons highlighted by neurofilament, right image), and increased proliferation (mean mitotic index 14.4 mitoses per 10 high power fields, n=15). Scale bar, 30 μm.

Figure 3. Comparison of clinical and genomic features of initial and recurrent tumor pairs. Summary of clinical and genomic tumor features from four patients with matched tumor tissue available from initial resection and subsequent recurrence (PXA#3, 6, 7) and from two different tumor recurrences (PXA#8) demonstrating changes in both single nucleotide variants and copy number alterations over time. After PXA # the i, denotes initial; r, denotes recurrent; and 1 or 2 denotes first or second recurrence. PXA#3i, 6i, 7r, and $8r^2$ are also included in Figure 1.

Figure 4. Intratumoral heterogeneity in anaplastic PXA. (**a**) Multiple distinct anatomic regions of PXA#4 were sampled and denoted A-F. These included A – anterior-inferior tip of mass, B – medial-inferior mass, C and D – adjacent central regions, E – lateral-posterior mass, and F – superior-lateral mass involving insular cortex. (**b**) Representative images from anatomically distinct regions (A, B, E, and F, from top to bottom) demonstrate mild to moderate variation in histologic appearance and Ki-67 labeling index. As regions C, D, and E were similar, representative images from region E are shown. Scale bar, 30 μm. (**c**) Copy number alterations compared between different regions demonstrate tumor heterogeneity. Uniform homozygous deletion of *CDKN2A* at chromosome 9p21 across regional tumor samples compared to representative normal germline (N). In contrast, there is a focal loss of interstitial chromosome 6q only in a subset of regions, (C, D, E). The color vertical line indicates the *CDKN2A* genomic position (left) and color shading indicate region of loss on chromosome 6q (right).

Samples have been grouped based on the presence (regions C, D, and E) or absence (regions A, F, and B) of the focal loss of interstitial chromosome 6q.

Table 1. Intratumoral heterogeneity of somatic genomic variants in anaplastic PXA.

Supplemental Figure 1. Recurrence-free survival and overall survival in patients with anaplastic PXA. Clinical follow-up was available for 12 of 15 patients with anaplastic PXA. **(a)** Analysis of overall survival was limited as median follow-up was 3.23 years (range 0.3-17.63 years) and two patients had died of their disease at follow-up. **(b)** A total of 92% (11/12) had recurred with a median progression-free survival from first diagnosis of 1.31 years (range 0.5-6.69 years). Censored data are denoted by black circle. The number of patients who underwent gross total resection (GTR), subtotal resection (STR), or for which the data was not available (N/A) are shown.

Supplemental Table 1. Summary of histologic and immunohistologic features of PXA cohort.

Supplemental Table 2. Genes targeted for sequencing on the UCSF500 Cancer Panel.

Supplemental Table 3. Structural variants identified in the PXA cohort.

Supplemental Table 4. Somatic single nucleotide variants (SNVs) and small insertions/deletions identified in the PXA cohort.

Supplemental Table 5. Somatic copy number alterations in the PXA cohort.

Supplemental Table 6. Intratumoral somatic single nucleotide variants (SNVs) identified in PXA#4.

Supplemental Table 7. Synopsis of PXA with or without anaplastic features investigated for *TERT* promoter mutations.

Supplemental Table 8. Association of *TERT* promoter mutation and anaplastic features in PXA.

Table 1. Intratumoral heterogeneity of somatic genomic variants in anaplastic PXA.

PXA#4-Sample	Gene	Variant	Transcript ID	Total Reads	Tumor variant allele frequency
A,B,C,D,E,F	*KEAP1*	KEAP1 p.V79D	NM_203500	>142	3-37%
B, F	*FOXO1*	FOXO1 p.S290P	NM_002015	>618	3-5%
B, F	*MGA*	MGA p.S1439P	NM_001080541	>357	7%
B, F	*TNC*	TNC p.T1469A	NM_002160	>638	6-7%
C	*SMARCA4*	SMARCA4 p.R448C	NM_001128844	91	4%
D	*CDK6*	CDK6 p.A162P	NM_001145306	511	7%
E	*ACVR1*	ACVR1 p.L8F	NM_001105	501	3%
E	*LRRK2*	LRRK2 p.P1072T	NM_198578	970	3%
E	*MCL1*	MCL1 p.K208E	NM_021960	852	3%
F	*POLD1*	POLD1 p.S434C	NM_001256849	241	6%

Figure 1, Phillips et al.

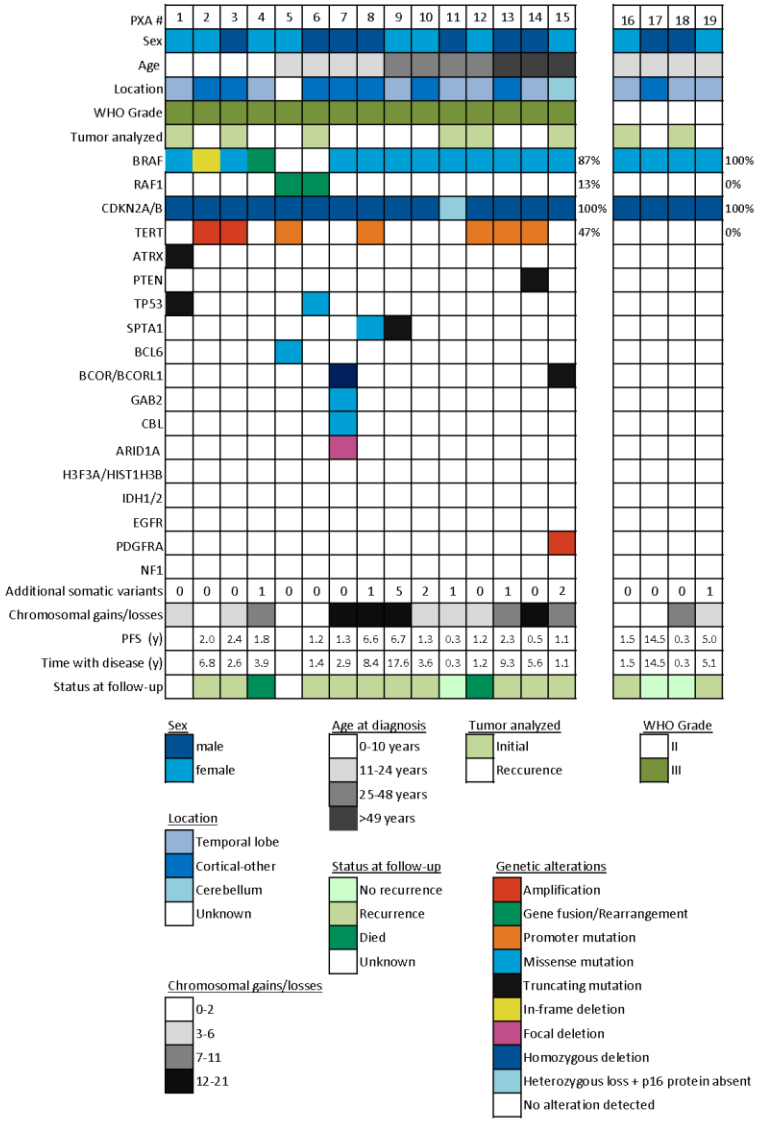

Figure 2, Phillips et al.

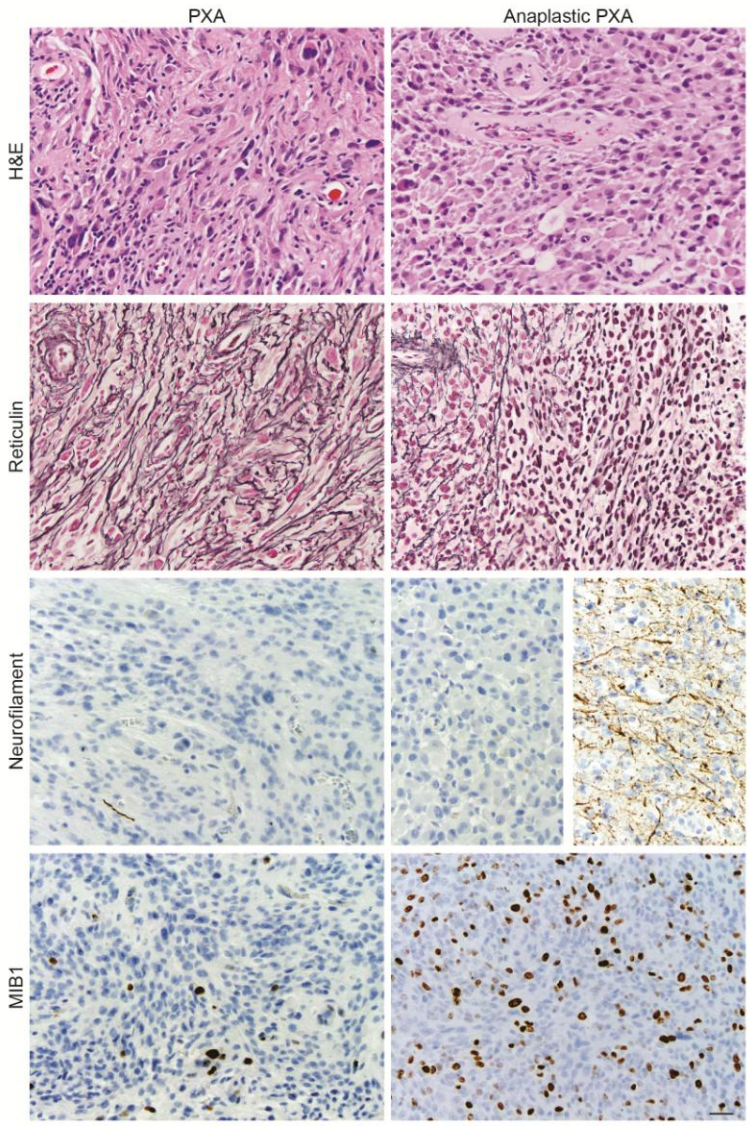

Figure 3, Phillips et al.

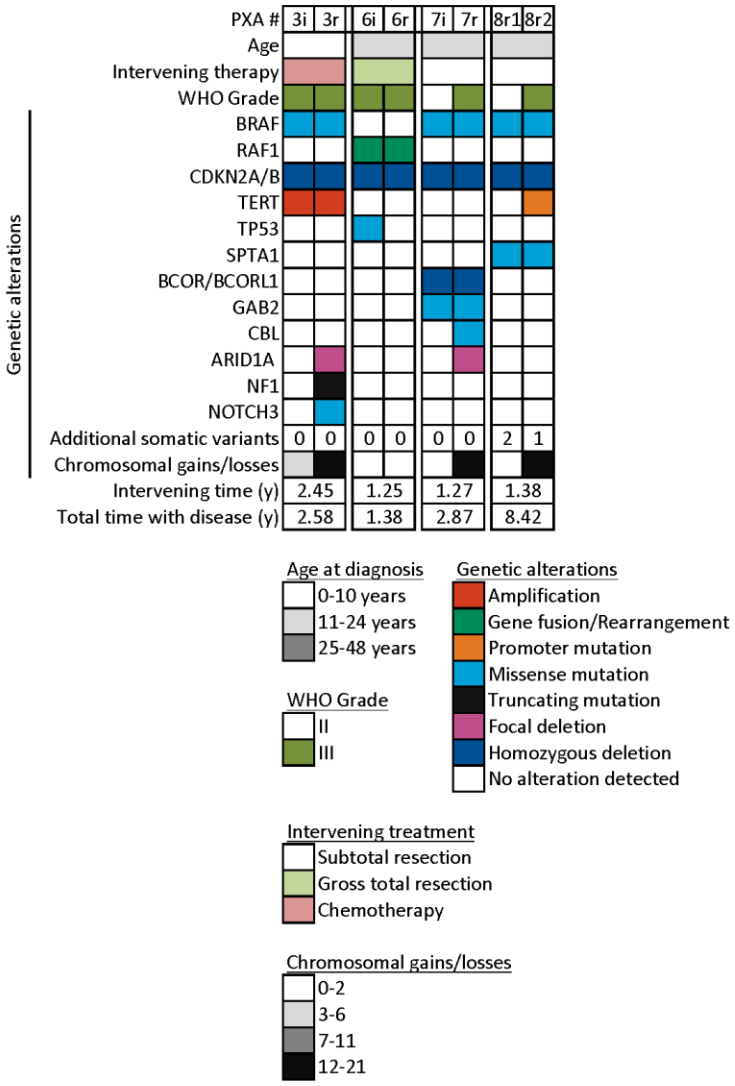

Figure 4, Phillips et al.